Journal of Materials Science and Engineering B 14 (1-3) (2024) 21-26
doi: 10.17265/2161-6221/2024.1-3.004

Electronic Structure Investigation of 12442 Iron-Based Superconductors Based on Block-Layer Model

Jianan Bian, Xinyuan Jiang, Yuchen Zou and Yiming Yu
School of Science, Jiliang University, Hangzhou 310018, China

Abstract: Superconducting transition temperature (T_c), as a crucial parameter, exploring its relationship with various macroscopic and microscopic factors helps to understand the mechanism of high-temperature superconductivity from multiple perspectives, aiding in a multidimensional comprehension of high-temperature superconductivity mechanisms. Drawing inspiration from the block-layer structure models of cuprate superconductors, we computationally investigated the interlayer interaction energies in the 12442-type iron-based superconducting materials $AkCa_2Fe_4As_4F_2$ (Ak = K, Rb, Cs) systems based on the block-layer model and explored their relationship with T_c. We observed that an increase in interlayer combinative energy leads to a decrease in T_c, while conversely, a decrease in interlayer combination energy results in an increase in T_c. Further, we found that the contribution of the Fe 3d band structure, especially the $3dz^2$ orbital, to charge transfer is significant.

Key words: Block-layer structural mode, iron-based superconductor, combinative energy, superconducting transition temperature.

1. Introduction

The unique properties of superconducting materials have found wide applications in both high and low electrical fields. Following the discoveries of cuprate and iron-based high-temperature superconductors [1-3], the exploration for novel high-temperature superconducting materials continues to intensify. Recent discussions have focused on intense debates concerning materials approaching room temperature superconductivity under strong high pressures [4-6], as well as the discovery of new nickel-based superconductors with T_c reaching over 80 degrees [7]. Theoretical and experimental studies have shown that microstructural variations in superconducting materials, such as ion heights, bond lengths, bond angles, interlayer distances, lattice matching, and pressure-induced microstructural changes, have an impact on the superconducting transition temperature [8-10]. Notably, in both cuprate and iron-based high-temperature superconductors, a block-layer model has been established based on the layer structure of superconductors, distinguishing between superconducting and charge reservoir block layers [11, 12]. Investigating the interlayer combination energy and its relationship with the superconducting transition temperature T_c holds particular significance in understanding high-temperature superconductivity. Intergrowth-structured iron-based superconductors [13] are newly synthesized self-doped iron-based superconducting materials designed based on a summary of the structural characteristics and basic structure types of iron-based superconductors. They are characterized by intergrowth structures. Their composition must meet certain conditions, such as lattice matching between block layers, charge transfer between block layers, and ordered occupation of the same (or similar) crystal positions by ions in different block layers. In recent years, a series of intergrowth-structured iron-based superconductors have been reported, such as the $AkAeFe_4As_4$ (Ak = K, Rb, Cs) 1144 system formed by intergrowth of $AkFe_2As_2$ and $AeFe_2As_2$, or the 12442 [14-18] system formed by inter growth of $AkFe_2As_2$ and 1111 LnFeAsO systems. The space group of the 12442 system is I4/mmm. Ln and Ak ions have significantly different radii, alternatingly

Corresponding author: Jianan Bian, M.S., research fields: condensed matter physics.

inserted between the Fe_2As_2 layers along the c-direction. In the $AkFe_2As_2$ of the 12442 system, the oxidation state of Fe is +2.5, while in the parent material $AeFe_2As_2$, the oxidation state of Fe is +2. Combining these, the formal oxidation state of Fe is +2.25, naturally satisfying charge transfer between block layers. It is evident that in the 12442 system, due to its prominent layer intergrowth structure, charge transfer between layers significantly influences superconducting properties. Inspired by the block-layer models of cuprate and iron-based superconductors and the essential features of intergrowth-structured iron-based superconductors, this study applies the block-layer model to the novel intergrowth-structured iron-based superconductors 12442 $AkCa_2Fe_4As_4F_2$ (Ak = K, Rb, Cs), distinguishing between superconducting and charge reservoir block layers. We compute the interlayer combination energy and investigate its relationship with the superconducting transition temperature T_c. Furthermore, through first-principles calculations of their electronic structures, especially the fine electronic structures of Fe 3d, we attempt to utilize the electronic structure and fine electronic structure of Fe 3d to explain the association between interlayer interaction energy and superconducting properties, exploring high-temperature superconductivity in intergrowth-structured iron-based superconductors from another novel perspective.

2. Experimental Setup

Based on DFT (density functional theory), crystal combination energy and interlayer combination energy were computed using the VASP (Vienna Ab-initio Simulation Package) software through Materials Studio modeling. The interaction between ions and electrons was described using the PAW (projector augmented wave) method, with a plane-wave cutoff energy of 400 eV, 8×8×1 *k*-point mesh for the 12442 system, and an energy convergence criterion set to 10^{-6} eV.

Referring to copper-based and iron-based superconductors, the calculation of the cohesive energy (E_{coh}) of 12442-type iron-based superconductors is performed as follows:

$$E_{coh} = E_n - E_0 \tag{1}$$

E_0 represents the total energy of the crystal, while E_n denotes the total energy of N constituent atoms in their isolated states. Subsequently, the 12442-type intergrowth superconductor is categorized into superconducting blocks and charge reservoir blocks (refer to Fig. 1). The interlayer combination energy is defined as the interaction energy between the superconducting block layers and the charge reservoir block layers within the superconductor, computed as follows:

$$E_{com} = E_{coh} - E_{pe} - E_{re} \tag{2}$$

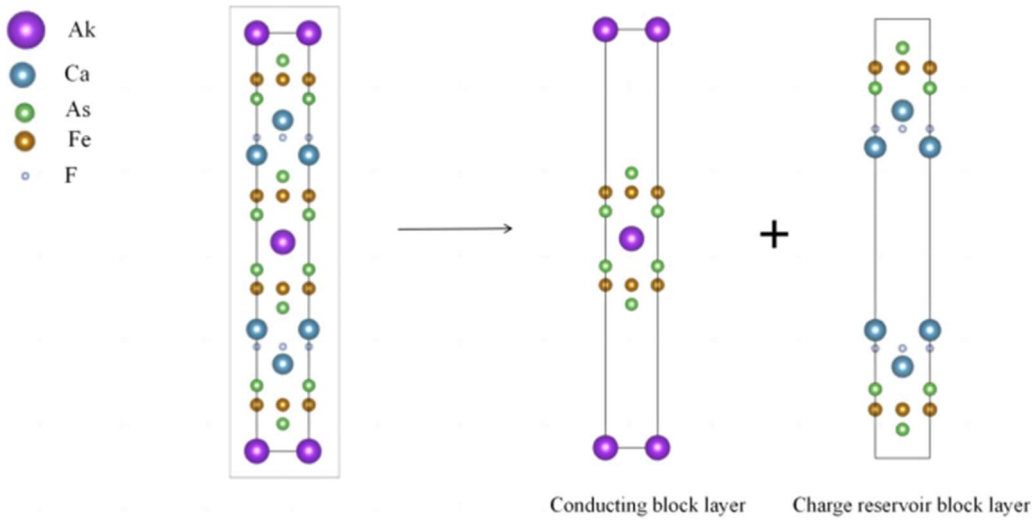

Fig. 1 Block-layer model for intergrowth structures of 12442 type iron-based superconductor.

The interlayer combination energy (E_{com}), the total combination energy of the cell (E_{coh}), the combination energy of the superconducting block (E_{pe}), and the combination energy of the charge reservoir block (E_{re}) have been defined.

3. Experimental Results

3.1 Crystal Combination Energy

Utilizing the established model and described computational methods, the crystal and interlayer combination energies of the 12442 system were calculated and analyzed. They were then compared with the superconducting transition temperature, T_c, as depicted in Fig. 2.

Fig. 2 illustrates the negative relationship between T_c and the interlayer combination energy in the $AkCa_2Fe_4As_4F_2$ (Ak = K, Rb, Cs) subclass of iron-based superconductors, where an increase in interlayer combination energy correlates with a decrease in T_c.

3.2 Electronic Structure

In this paper, the calculations reveal that the antiferromagnetic state is more stable, albeit with minimal impact on energy. Building upon this, band structures and DOSs (density of states) under the antiferromagnetic state were computed. In Figs. 3-5a, band analysis indicates that for the superconducting materials $AkCa_2Fe_4As_4F_2$ (Ak = K, Rb, Cs), eight bands intersect the Fermi surface along the paths Γ-X-M-Γ-Z-R-A-Z, all exhibiting dense cylindrical hole-like pockets at the M and Γ points. Near the Fermi surface at the M point, there are eight electron pockets, while at the Γ point, there are eight hole-like pockets.

From the projected band structure in Figs. 3-5a, it is evident that the dz^2 orbital of Fe exhibits the most crossings with the Fermi surface, occurring at Γ-X, M-Γ, and Z-R. Consequently, among the five orbital bands, the dz^2 orbital exerts the most significant influence on its properties. In general, the band structures of the five suborbitals of Fe 3d in the eight superconductors share three prominent features:

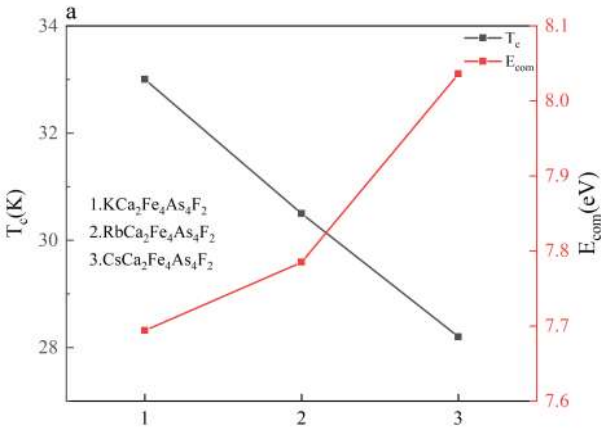

Fig. 2 Combination energy between blocks of 12442 intergrowth structures' relationship with T_c.

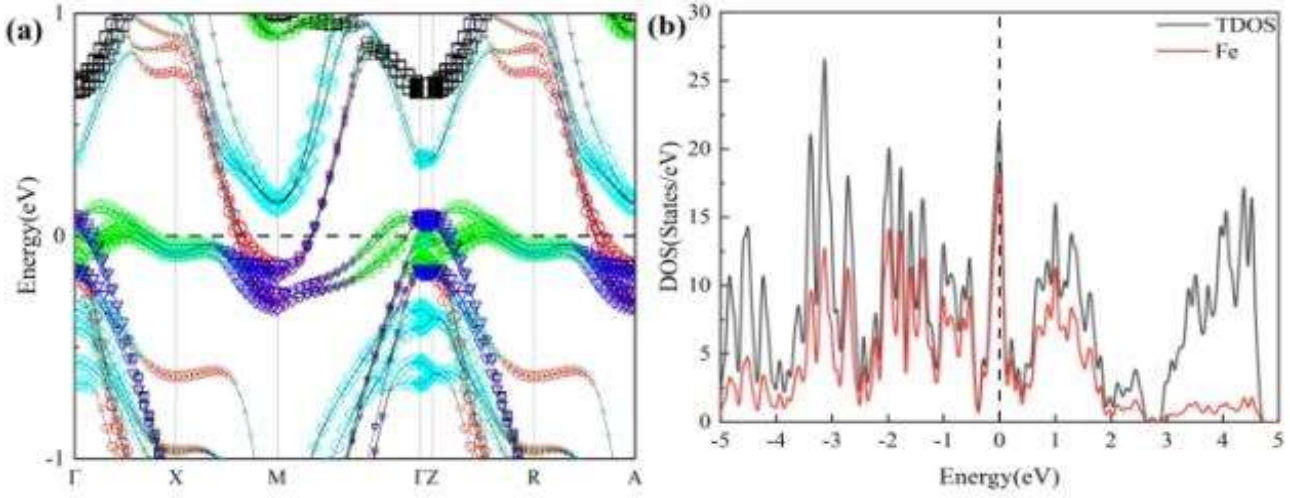

Fig. 3 DOS and fine band structure of Fe 3d of $KCa_2Fe_4As_4F_2$.

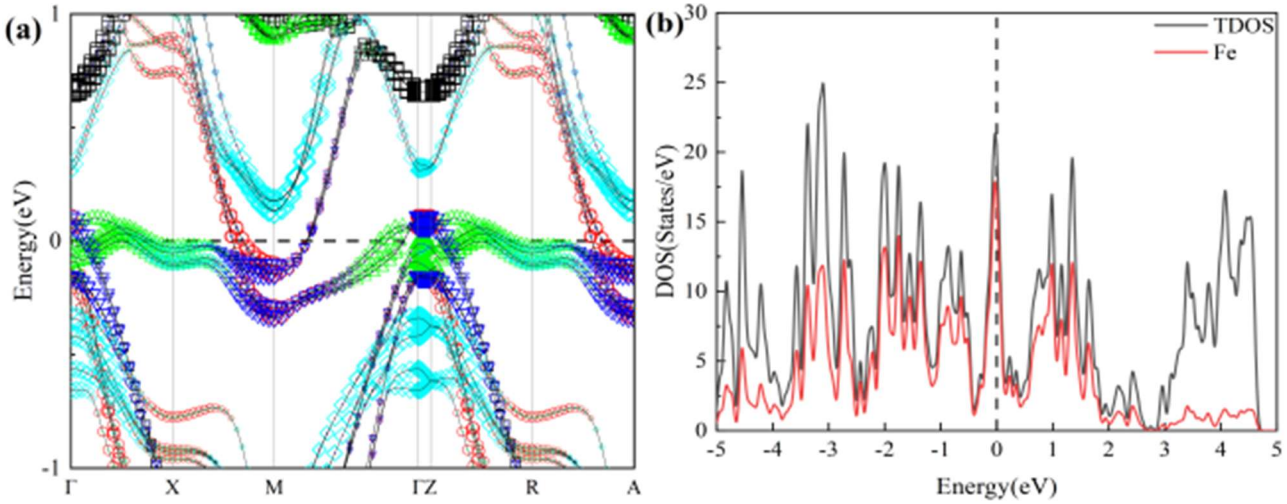

Fig. 4 DOS and fine band structure of Fe 3d of $RbCa_2Fe_4As_4F_2$.

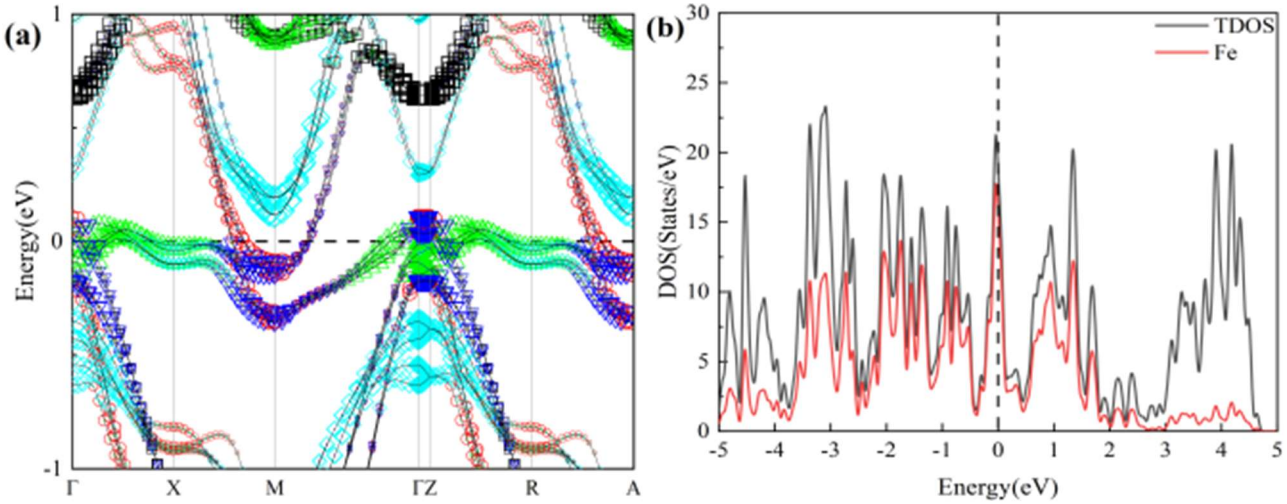

Fig. 5 DOS and fine band structure of Fe 3d of $CsCa_2Fe_4As_4F_2$.

(1) Along the Γ-Z path, flat bands are observed, with the dxz, dyz, and dz^2 orbitals particularly evident. Notably, the dz^2 orbital exhibits eight small flat segments near the Fermi surface from 0.05 to 0.1 eV and -0.2 to -0.15 eV, which are closely associated with superconductivity in iron-based superconductors and warrant attention.

(2) The dz^2 orbital is the closest to the Fermi surface and crosses it most frequently, exerting a significant influence on T_c.

(3) Along the X-M path, several suborbitals intersect near the Fermi surface from -0.2 to -0.1 eV. It is evident that among the five suborbitals of Fe 3d, those contributing the most to the Fermi surface and having a stronger impact on T_c are the dxz, dyz, and dz^2 orbitals of Fe. Particularly, the dz^2 orbital has the most significant influence on the Fermi surface of 12442 materials, reflecting the coupling between layers along the z-direction and interlayer charge transfer, which correlates with the superconducting transition temperature. Therefore, the interlayer interaction energy calculated based on the block-layer model is correlated with T_c, providing a sound explanation from the electronic structure of the crystal.

Figs. 3-5b show the DOSs for 12442, from which it is observed that the Fermi surface exhibits the largest contribution from Fe. For ease of comparing the electronic structures among different materials,

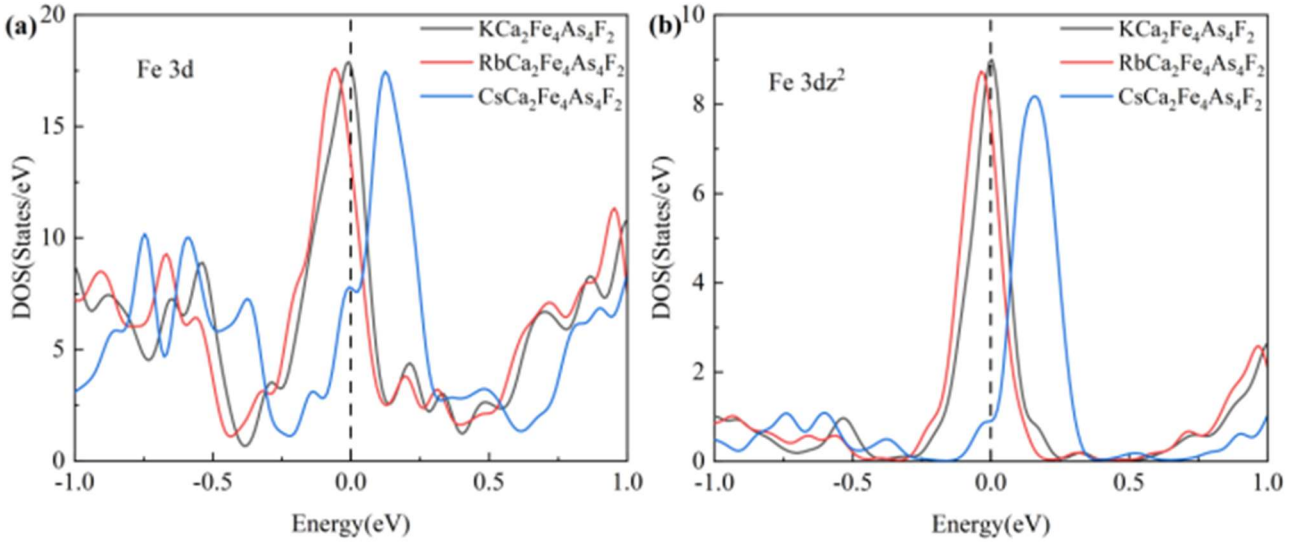

Fig. 6 Comparison of DOSs of Fe 3d and dz^2 in $AkCa_2Fe_4As_4F_2$ (Ak = K, Rb, Cs) system.

Figs. 6a and 6b respectively present the DOS comparison of Fe's 3d orbitals and dz^2 orbitals in the $AkCa_2Fe_4As_2F_2$ and 12442 systems. From Fig. 6a, it is observed that there are distinctions in the DOS contributions of Fe's 3d orbitals among the $AkCa_2Fe_4As_2F_2$ superconductors. Specifically, the DOS peak of $KCa_2Fe_4As_2F_2$ is larger and closer to the Fermi surface compared to others. While the DOS peak positions of $RbCa_2Fe_4As_2F_2$ and $CsCa_2Fe_4As_2F_2$ are closer to $KCa_2Fe_4As_2F_2$, they gradually decrease in peak height and move further from the Fermi surface, resulting in electron numbers near the Fermi surface satisfying $KCa_2Fe_4As_2F_2$ > $RbCa_2Fe_4As_2F_2$ > $CsCa_2Fe_4As_2F_2$. This relationship aligns with our previous speculation, suggesting that interlayer interactions between the two blocks influence charge transport. Considering the formula relating the Fermi surface DOSs (N(EF)) to T_c in the BCS (Bardeen-Cooper-Schrieffer) theory, it is evident that N(EF) and T_c in the 12442 system do not adhere to this relationship, indicating that 12442 superconductors do not conform to conventional superconductors according to the BCS theory. Considering our qualitative exploration of the relationship between interlayer combination energy and T_c through electronic band interpretation, Fe's $3dz^2$ orbital better reflects the interaction between block layers along the z-direction. Therefore, we primarily compare the influence of the dz^2 DOSs among the five superconducting materials. In summary, for the 12442 layer iron-based superconducting structures, through comparative analysis of band structures and DOSs of each element, it is evident that Fe's 3d orbital electrons exert a decisive influence on the Fermi surface and superconducting properties. Furthermore, through detailed analysis of the fine bands and DOSs of Fe's five suborbitals, it is revealed that electrons in Fe's dz^2 suborbital play a crucial role in the Fermi surface and superconducting properties, reflecting the coupling between block layers along the z-direction and interlayer charge transfer, which correlates with the superconducting transition temperature. The presence of interlayer combination energy affects charge transfer, thus the interlayer interaction energy calculated based on the block-layer model correlates with T_c, providing a sound explanation from the electronic structure of the crystal.

4. Conclusions

This paper systematically investigates the interlayer combination energy, band structure, and DOSs of the 12442 layer iron-based superconducting systems $AkCa_2Fe_4As_4F_2$ (Ak = K, Rb, Cs) through theoretical

calculations. The following conclusions are drawn: Following the block-layer model of copper-based and iron-based superconductors, it is observed that in the 12442 layer iron-based superconductors $AkCa_2Fe_4As_4F_2$, larger interlayer combination energies correspond to lower T_c, while smaller interlayer interactions lead to higher T_c, consistent with the conclusions for the 1144 systems. Fe's 3d orbitals predominantly contribute near the Fermi level, with the dxz, dyz, and dz^2 orbitals exhibiting the highest contributions among Fe's five orbitals. Among them, the dz^2 orbital plays a crucial role in interlayer charge transfer.

Based on these research findings, it is concluded in this chapter that the relationship between interlayer combination energy and T_c exists in the 12442 layer iron-based superconductors $AkCa_2Fe_4As_4F_2$ similar to cuprate superconductors.

References

[1] Kamihara, Y., Watanabe, T., Hirano, M., and Hosono, H. 2008. "Iron-Based Layered Superconductor La[$O_{1-x}F_x$]FeAs (x = 0.05-0.12) with T_c = 26 K." *Journal of the American Chemical Society* 130 (11): 3296-7.

[2] Chen, X. H., Wu, T., Wu, G., Liu, R. H., Chen, H., and Fang, D. F. 2008. "Superconductivity at 43 K in $SmFeAsO_{1-x}F_x$." *Nature* 453 (7196): 761-2.

[3] Aravinda, M., Kini, U., Geiser, H., Chuen, I., and Kao, K. 1987. "Superconductivity at 91 K in the Magnetic Oxide Holmium Barium Copper Oxide, $HoBa_2Cu_3O_{6+x}$." *Inorganic Chemistry* 26 (11): 1645-6.

[4] Ming, X., Zhang, Y. J., Zhu, X. Y., Li, Q., He, C. P., Liu, Y. C., Huang, T. H., Liu, G., Zheng, B., Yang, H., Sun, J., Xi, X. X., and Wen, H. H. 2023. "Absence of Near-Ambient Superconductivity in $LuH_{2\pm x}N_y$." *Nature* 620: 72-7.

[5] Griffin, S. M. 2023. "Origin of Correlated Isolated Flat Bands in Copper-Substituted Lead Phosphate Apatite." http://arxiv.org/pdf/2307.16892.

[6] Sun, H. L., Huo, M. W., Hum, X. W., Li, J. Y., Liu, Z. J., Han, Y. F., Tang, L. Y., Mao, Z. Q., Yang, P. T., Wang, B., Cheng, J. G., Yao, D. X., Zhang, G. M., and Wang, M. 2023. "Signatures of Superconductivity near 80 K in a Nickelate under High Pressure." *Nature* 621 (7979): 493-8.

[7] Mizuguchi, Y., Hara, Y., Deguchi, L., Tsuda, S., Yamaguchi, T., Takeda, K., Kotegawa, H., Tou, H., and Takano, Y. 2010. "Anion Height Dependence of T_c for the Fe-Based Superconductor." *Superconductor Science and Technology* 23: 054013.

[8] Zhao, J., Huang, Q., Cruz, C., Li, S. L., Lynn, J. W., Chen, Y., Green, M. A., Che, G. F., Li, G., and Li, Z. 2008. "Structural and Magnetic Phase Diagram of $CeFeAsO_{1-x}F_x$ and Its Relation to High-Temperature Superconductivity." *Nature Materials* 7 (12): 953-9.

[9] Lee, C. H., Iyo, A., Eisaki, H., Kito, H., Fernandez-Diaz, M. T., Ito, T., Kihou, K., Matsuhata, H., Braden, M., and Yamada, K. 2008. "Effect of Structural Parameters on Superconductivity in Fluorine-Free $LnFeAsO_{1-y}$ (Ln = La, Nd)." *J. Phys. Soc. Jpn*. 77: 08370.

[10] Zhang, H., Cheng, L. L., and Zhao, Y. 2000. "Calculation of Combinative Energy between Perovskite and Rocksalt Blocks in YBa2Cu3O7-δ." *Physical Review B* 62: 121.

[11] Wang S X, Zhang H. 2003. "Interaction between Two Structural Blocks and Superconductivity in $La_{2-x}M_xCuO_4$ (M= Ba, Sr)." *Physical Review B* 68(1): 012503.

[12] Zhang, L., Li, Y. K., Tao, Q., Shi, S. L., Wang, X. Y., and Zhou, Y. 2010. "Interaction between Two Structural Blocks and Its Correlation with Superconductivity in $SmFeAsO_{1-x}F_x$ and $SmFe_{1-x}M_xAsO$ (M=Co, Ni)." *Europhysics Letter* 91 (5): 56005.

[13] Wang, Z. C., and Cao, G. H. 2018. "Self-doped iron-based superconductors with intergrowth structures." *Acta Physica Sinica* 67 (20): 142-157.

[14] Yi, X., Li, M., Xing, X., Meng, Y., Zhao, C., and Shi, Z. 2020. "Single Crystal Growth and Effects of Ni Doping on the Novel 12442-Type Iron-Based Superconductor $RbCa_2Fe_4As_4F_2$." *New Journal of Physics* 22 (7): 073007.

[15] Huang, Y. Y., Wang, Z. C., Yu, Y. J., Ni, J. M., and Li, S. Y. 2019. "Multigap Nodeless Superconductivity in $CsCa_2Fe_4As_4F_2$ Probed by Heat Transport." *Physical Review B* 99.020502.

[16] Huang, Y. N., Ye, Z. F., Liu, D. Y., and Qiu, H. Q. 2023. "Role of Lanthanide in the Electronic Properties of $RbLn_2Fe_4As_4O_2$ (Ln=Sm and Ho) Superconductors." *Chinese Physics Letters* 40 (9): 101-6.

[17] Wang, Z. C., He, C. Y., Tang, Z. T., Wu, S. Q., and Cao, G. H. 2017. "Synthesis, Crystal Structure and Superconductivity in RbLn2Fe4As4O2 (Ln = Sm, Tb, Dy, and Ho)." *Sci. China: Mater*. 60: 83.

[18] Wang, Z. C., He, C. Y., Wu, S. Q., Tang, Z. T., Liu, Y., and Cao, G. H. 2017. "Synthesis, Crystal Structure and Superconductivity in RbLn2Fe4As4O2 (Ln = Sm, Tb, Dy, and Ho)." *Synthesis Chem. Mater*. 29: 1805.